Int. J. Electrochem. Sci., 12 **(2017)** 2344 – 2352, doi: 10.20964/2017.03.41

International Journal of
ELECTROCHEMICAL
SCIENCE
www.electrochemsci.org

Short Communication

Electrodeposition and Anodization of Al-TiO_2 Composite Coatings for Enhanced Photocatalytic Activity

Masao Miyake[*], *Ayumu Takahashi, Tetsuji Hirato*

Graduate School of Energy Science, Kyoto University, Yoshida-honmachi, Sakyo-ku, Kyoto 606-8501, Japan
[*]E-mail: miyake.masao.4e@kyoto-u.ac.jp

Received: 25 November 2016 / *Accepted:* 11 January 2017 / *Published:* 12 February 2017

In this study, we investigated the feasibility of a new process for the fabrication of Al-based composite coatings containing TiO_2 particles with high photocatalytic activity. In the first step of this process, Al-TiO_2 composite coatings were electrodeposited in a dimethyl sulfone–aluminum chloride bath with suspended TiO_2 particles yielding Al-matrix composite coatings with uniformly dispersed TiO_2 particles. Subsequently, the electrodeposited Al-TiO_2 composite coatings were anodized in oxalic aqueous solution. Through this anodization step, the Al matrix was converted into an alumina layer with many nanopores extending from the surface of the coating toward the substrate. As a consequence, a porous alumina layer supporting TiO_2 particles was formed. The photocatalytic activity of the anodized composite coatings was confirmed to be higher than that of the as-deposited coatings.

Keywords: composite electrodeposition; composite electroplating; aluminum electrodeposition; anodization; photocatalyst

1. INTRODUCTION

Aluminum coatings are well known to have excellent physicochemical properties, including high corrosion resistance, high conductivity, and low density, and are thus used in a wide range of industrial applications, from construction materials to electronic components. While various techniques are available for the preparation of Al coatings, electrodeposition is attracting growing interest because complex-shaped objects can be coated evenly, the deposition rate is relatively high, and the coating thickness can be easily controlled. Although the electrodeposition of Al is not feasible in aqueous solution, it is possible in certain non-aqueous media such as molten salts [1, 2], organic solvents [3-9], and ionic liquids [10-18].

The electrodeposition of metal matrix composite coatings containing ceramic particles has been investigated with the aim of obtaining coatings with additional functionalities [19]. The enhancement of mechanical properties, such as hardness and wear resistance, by incorporating inert ceramic particles such as SiO_2, Al_2O_3, and SiC has been extensively studied [20]. Composites containing TiO_2 particles are of great interest, because they exhibit not only improved mechanical properties [21-24], but also photocatalytic and photoelectrochemical behavior, by taking advantage of the excellent photocatalytic ability of TiO_2 [25-30]. Al-TiO_2 composite coatings can be potentially used, for example, as high corrosion-resistance coatings having a photo-induced self-cleaning function. The photo-induced self-cleaning behavior of metal matrix composite coatings has already been demonstrated for Ni-TiO_2 coatings [27].

However, simple composite coatings composed of a metal matrix and uniformly dispersed TiO_2 particles may not exhibit strong photocatalytic properties, as most of the TiO_2 particles in the coatings are enclosed by the metal matrix and cannot thus exert their photocatalytic activity. Only the particles exposed on the surface of the coating can catalyze reactions. One possible approach to enhance the photocatalytic activity of composite coatings is to make the matrix a porous one, so that reactants can be in contact with the TiO_2 particles located deep inside the coating. For Al matrices, a well-known anodizing process [31, 32] can be used to convert solid Al matrices into porous alumina layers. The typical porous anodic alumina layers grown from bulk aluminum comprise a hexagonal array of cells with cylindrical pores, with the cell walls composed of alumina. The pore diameter and interpore distance vary in the range of 10–400 nm and 50–600 nm, respectively, depending on the anodization conditions [31, 32]. If a porous structure is formed in the Al matrix of the composite by anodization, reactants should be able to reach the TiO_2 particles through the pores. Furthermore, unlike the Al metal, alumina exhibits transparency to UV light and, thus, UV light can also reach the TiO_2 particles inside the coating. Therefore, it is expected that the photocatalytic activity of Al-TiO_2 composites will be enhanced after anodization. However, to the best of our knowledge, the study on the anodization of Al-TiO_2 composites has not been reported.

Here, we propose a new process for the formation of Al-base composite coatings showing high photocatalytic activity. The process is summarized schematically in Fig. 1. In this process, an Al-TiO_2 composite coating is electrodeposited, and then the coating is anodized to convert the Al matrix into porous alumina. In previous studies, we demonstrated the electrodeposition of Al in a dimethyl sulfone ($DMSO_2$)–aluminum chloride system. Dense Al coatings can be electrodeposited in a $DMSO_2$–$AlCl_3$ bath at ~110 °C with a current efficiency of >95% [3-8]. The co-deposition of SiO_2, SiC, TiB_2, and BN particles with Al in $DMSO_2$–$AlCl_3$ baths has also been demonstrated [33, 34]. In this study, we have prepared Al-TiO_2 composite coatings using a $DMSO_2$–$AlCl_3$ bath with suspended TiO_2 particles. As for the Al matrix composites, some research groups have studied the anodization of composites containing ceramic (SiC, AlN, and Al_2O_3) particles prepared by liquid metal infiltration and powder metallurgy methods [35-40] with the aim to improve the corrosion resistance and wear resistance of the composites. These studies show that porous anodic alumina layers can be formed on the composites even when inert particles are present in the Al matrix. However, the detailed porous structure formed on the composites has not been well studied. It is therefore unclear whether the photocatalytic activity of Al-TiO_2 composite coatings will be maintained and/or improved by

anodization treatments. In this study, the electrodeposited Al-TiO_2 composite coatings were anodized, and the effect of anodization on the photocatalytic activity of the coatings was investigated.

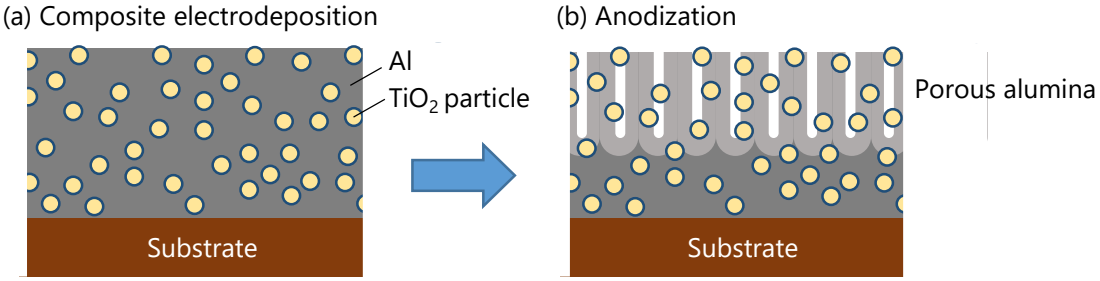

Figure 1. Schematic representation of the formation of photocatalytic Al-base composite coatings containing TiO_2 particles. The process comprises (a) the composite electrodeposition of an Al coating containing TiO_2 particles, and (b) the subsequent anodization of the Al-TiO_2 coating to convert the solid Al matrix into a porous alumina layer.

2. EXPERIMENTAL

2.1 Electrodeposition

The electrolytic bath was prepared in an Ar-filled glove box equipped with a circulation system, where the electrodeposition of Al and Al-TiO_2 composite coatings was carried out. The electrolytic bath for the electrodeposition of Al was prepared by mixing $DMSO_2$ (Tokyo Chemical Industry) and anhydrous $AlCl_3$ grains (Fluka, crystallized, 99%) at a molar ratio of 10:2. $DMSO_2$ was used after drying for >24 h under reduced pressure at 60 °C. $AlCl_3$ was used as received and stored in a glove box. Anatase TiO_2 powder (Titan Kogyo, ST-11) was added to the $DMSO_2$–$AlCl_3$ bath for the electrodeposition of Al-TiO_2 composite coatings. TiO_2 powder was used as received without any pre-treatment. A copper plate and an aluminum plate were used as the substrate and counter electrodes, respectively. Part of the copper plate was covered with PTFE tape so that only a certain area (20 × 20 mm^2) was exposed. Electrodeposition was carried out galvanostatically at 60 mA cm^{-2} and 110 °C for 0.5 h. Prior to electrodeposition, the bath with the TiO_2 powder underwent sonication with a ultrasonic homogenizer (As-one, Sonicstar85) for >5 min. During electrodeposition, the bath was stirred with a magnetic stirrer and a stirrer-follower bar (20 mm × 5 mm) at 100 rpm. After electrodeposition, the Al and Al-TiO_2 coatings were taken out of the glove box and washed with distilled water.

2.2 Anodization and etching

The electrodeposited Al-TiO_2 coatings were anodized in a 0.3 M oxalic acid aqueous solution at 40 V and 30 °C using a Pt sheet as the counter electrode. Some of the anodized coatings were further chemically etched or pore-widening etched in 5 wt% aqueous phosphoric acid for 20 min. The Cu substrate was kept masked with PTFE tape to prevent the substrate from dissolving into the solution.

2.3 Characterization

Scanning electron microscopy (SEM; S-3500, Hitachi) in combination with energy-dispersive X-ray spectroscopy (EDX; INCAxact, Oxford Instruments) were used to observe the morphology and measure the elemental composition of the coatings. The volume fraction of TiO_2 in the Al-TiO_2 composite coatings was calculated from the value of the Ti/Al content ratio as determined by EDX on the basis of the densities of anatase TiO_2 and Al (3.9 and 2.7 g cm^{-3}, respectively). A field-emission scanning electron microscope (FE-SEM; Hitachi, SU6600) was used to obtain images of the TiO_2 powder and the coatings. For coating cross-section observation, electrodeposition was performed on a 100 nm thick Cu film sputtered on a glass substrate and, then, the cross-section was obtained by fracturing the glass substrate.

The photocatalytic activity was evaluated through the photodegradation of methylene blue (MB) in aqueous solution. An Al-TiO_2 composite coating with an area of 20 × 20 mm^2 on the Cu substrate was placed in a 4 μM MB solution (3 mL) and irradiated with a UV lamp at a central wavelength of 365 nm (Optocode, FL 365-SD). The concentration of MB was determined from the optical absorbance of the solution at 664 nm as per Beer's law. The optical absorption spectrum of the solution was measured employing a spectrophotometer (Shimadzu, UV-2450).

3. RESULTS AND DISCUSSION

3.1 Electrodeposition of Al-TiO_2 composite coatings

Al-TiO_2 composite coatings were electrodeposited in a $DMSO_2$–$AlCl_3$ bath with suspended TiO_2 powder. Figure 2 presents the SEM images of the TiO_2 powder used for electrodeposition, showing that the powder is composed of particles with a mean size of 0.65 ± 0.32 μm. The higher magnification image (Fig. 2b) reveals that each particle is an aggregate of smaller, primary particles of ~20 nm, which is in agreement with the estimation from the peak width of XRD signals. The primary particles could not be separated into their dispersed form even when sonication was applied, resulting in white turbidity of the bath containing the TiO_2 powder. The particles seemed to retain their aggregate form in the bath.

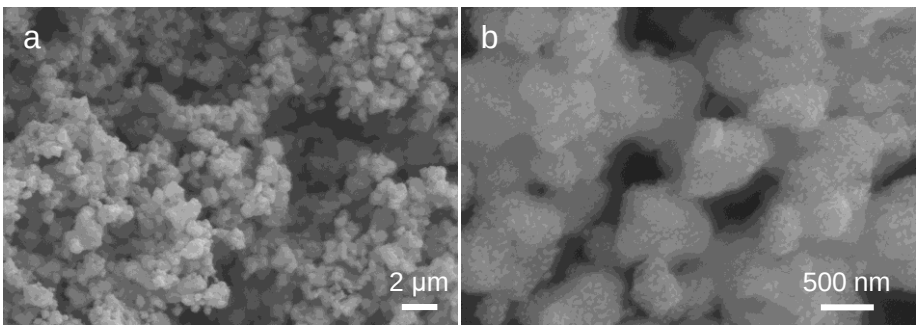

Figure 2. SEM images of the TiO_2 powder used in the composite electrodeposition.

Galvanostatic electrodeposition at 60 mA cm^{-2} in the bath containing the TiO_2 powder yielded Al-TiO_2 composite coatings with gray appearance. Figure 3 presents the SEM images of a typical composite coating obtained in this study. The surface SEM image (Fig. 3a) shows that TiO_2 particles with 0.3–1 μm in size are uniformly dispersed across the surface of Al deposits, which are composed of faceted grains with 1–2 μm in size. The higher magnification image of the surface (Fig. 3b) reveals that the TiO_2 particles in the coating are aggregates of smaller particles. Thus, the morphology of the TiO_2 particles remains intact after they are added to the bath for electrodeposition (Fig. 2). In the image, some TiO_2 particles appear half embedded in the Al grains, not just attached on their surface. The image of the fractured cross-section (Fig. 3c) reveals the formation of a composite coating with a thickness of ~40 μm. In the higher magnification image (Fig. 3d), TiO_2 particles embedded in the Al deposit can be observed. The homogeneous dispersion of TiO_2 particles across the cross-section was thus confirmed.

The TiO_2 content of the coating electrodeposited in the bath containing 2 g L^{-1} TiO_2 was 8 vol%, and it increased up to ~32 vol% almost proportionally to the amount of TiO_2 added to the bath. However, the TiO_2 content seemed to reach saturation at ~30 vol% for TiO_2 concentrations higher than 10 g L^{-1}. This TiO_2 content of ~30 vol.% is higher than that of other metal matrix-TiO_2 composite coatings electrodeposited from aqueous solutions (10–15 vol.% [23, 24, 27, 28]). The higher degree of the TiO_2 codeposition in this study should be ascribable to the use of the organic bath [33].

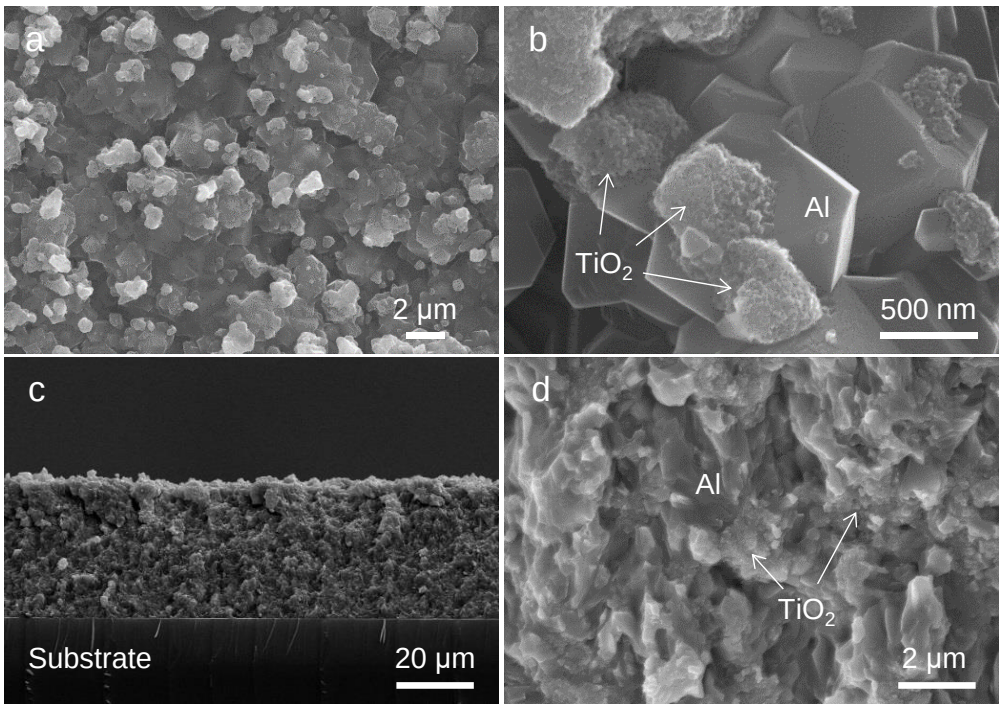

Figure 3. SEM images of (a, b) the surface and (c, d) fractured cross-section of an Al-TiO_2 composite coating electrodeposited in a bath containing 2 g L^{-1} TiO_2. The TiO_2 content of the coating was 8 vol%.

3.2 Anodization of Al-TiO_2 composite coatings

The Al-TiO_2 composite coatings were anodized in oxalic acid at 40 V. Figure 4 presents SEM images of the surface of a composite coating (8 vol% TiO_2) after anodization. Comparison of the images before and after anodization (Fig. 3a and Fig. 4a) reveals that the surface morphology of the coating at low magnification does not change significantly after anodization. The image at high magnification confirms the presence of TiO_2 particles embedded on the surface even after anodization and, more importantly, the image reveals the formation of many pores on the surface of the Al grains. The diameter and spacing of the pores are about 20 nm and 80 nm, respectively, which are comparable to the values reported for pores formed in highly pure Al sheets by anodization under the same conditions [41].

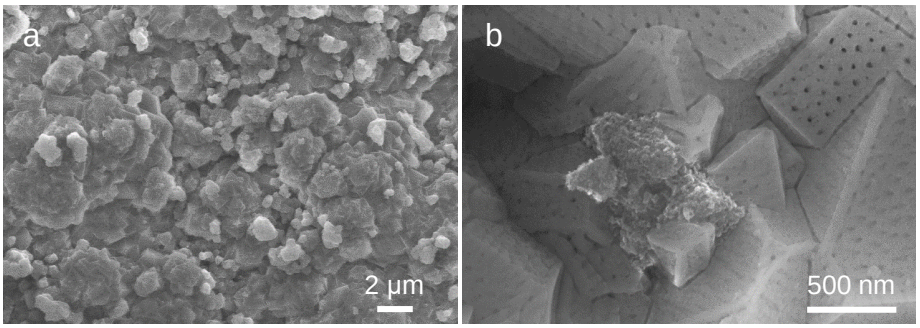

Figure 4. SEM images of the surface of the Al-TiO_2 composite coating containing 8 vol% TiO_2 after anodization.

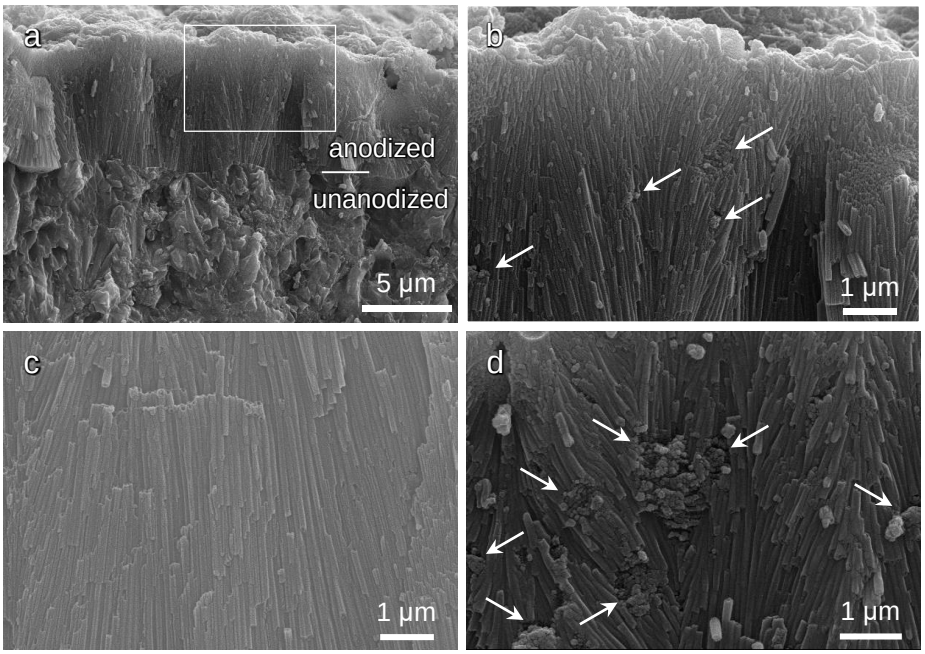

Figure 5. SEM images of fractured cross-sections of the Al-TiO_2 composite coatings containing (a, b) 4, (c) 2, and (d) 8 vol% TiO_2 after anodization for 0.5 h. Image (b) is a higher magnification of the framed area in (a). The arrows indicate the TiO_2 particles in the anodized layer.

Figure 5 presents the SEM images of the fractured cross-sections of coatings after anodization. As can be seen in the low magnification image shown in Fig. 5a, an anodized layer with a thickness of ~7 μm was formed on the surface of the composite coating with 4 vol% TiO_2 after anodization for 30 min. The high magnification images (Figs. 5b–5d) show pores extending in the direction towards the substrate on the whole anodized layer. The presence of TiO_2 particles in the porous anodized layer can also be confirmed from these images. Figures 5c and 5d show the pore structures generated in the coatings with different TiO_2 contents for comparison. The pores in the coating with a low TiO_2 content (2 vol%) extend straight down towards the substrate (Fig. 5c). This pore structure is similar to that typically observed in anodized layers formed on pure Al sheets under similar conditions [42]. In comparison, the pores observed in the composite with high TiO_2 content (8 vol%) are somewhat curved, because the TiO_2 particles interfere with the pore growth (Fig. 5d). However, although the TiO_2 particles in the coatings interfere with pore growth, the images clearly show that the Al matrix can still be converted into a porous alumina layer and, therefore, a porous alumina layer with TiO_2 particles is formed.

After anodization, the coatings underwent chemical etching, the so-called pore-widening etching, in a 5 wt% H_3PO_4 aqueous solution at room temperature for 20 min. It is known that alumina is etched at a rate of ~8 nm per hour under these conditions [43]. Therefore, the pore diameter should be increased after etching, while the porous structure of the anodized layer is retained as a whole.

3.3 Photocatalytic activity

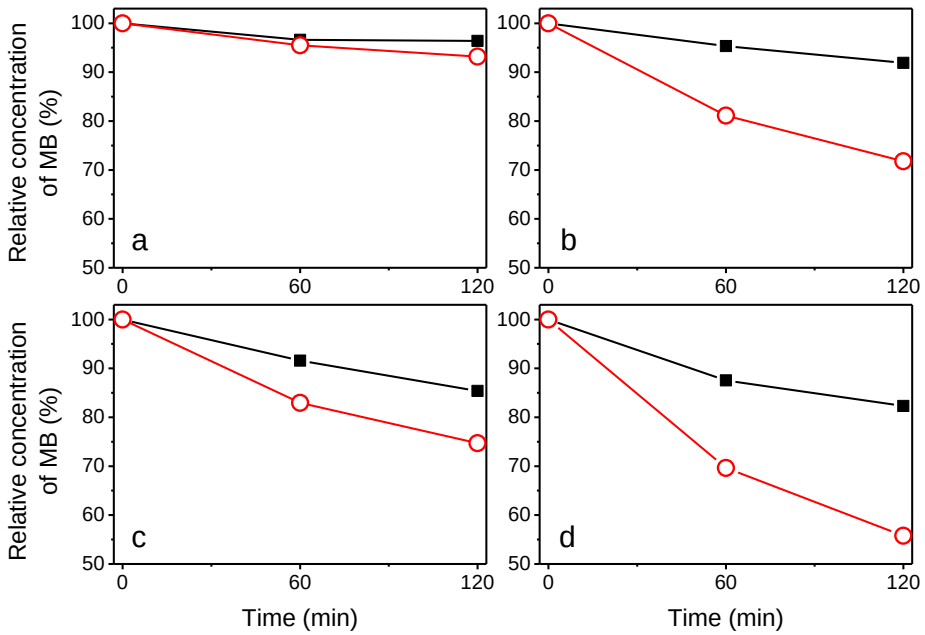

Figure 6. Variation of the concentration of MB in aqueous solution in contact with Al and composite coatings containing (a) 0, (b) 8, (c) 17, and (d) 32 vol% TiO_2. The closed squares and open circles refer to data for the as-electrodeposited and anodized coatings, respectively.

The effect of anodization on the photocatalytic activity of the coatings was examined by measuring the photodegradation rate of MB aqueous solutions [44] in contact with the as-deposited or anodized coatings. For comparison, the same measurements were carried out with an electrodeposited Al coating containing no TiO_2 particles. Figure 6 shows the variation in the MB concentration of the solutions in contact with coatings containing 0, 8, 17, and 32 vol% TiO_2 under UV irradiation. Before anodization, comparison of the degradation rates of MB for the coatings with different TiO_2 contents (closed squares) confirmed that the photodegradation rate of MB, i.e. the photocatalytic activity of the coating, tended to increase with the increasing TiO_2 content. Comparison of the data for the as-deposited (closed squares) and anodized (open circles) coatings revealed that the photocatalytic activity significantly increases after anodization for every composite coating with TiO_2 particles (Figs. 6b–d). In contrast, only a small difference, within experimental error, was observed for the photodegradation rate of MB in contact with the Al coating without TiO_2 particles (Fig. 6a). These results indicate that the photocatalytic activity of the composite coatings increased because the number of TiO_2 particles which can catalyze the reaction was increased by the formation of the porous structure.

4. CONCLUSIONS

Electrodeposition of Al in a $DMSO_2$–$AlCl_3$ bath with suspended TiO_2 powder afforded Al matrix composite coatings containing uniformly dispersed TiO_2 particles. The composite coatings could be anodized in oxalic acid solution, and porous alumina layers containing different amounts of TiO_2 particles were successfully formed. The photocatalytic activity of the composite coatings was found to be enhanced by anodization treatment.

References

1. M. Jafarian, M. G. Mahjani, F. Gobal and I. Danaee, *J Appl Electrochem*, 36 (2006) 1169.
2. M. Jafarian, F. Gobal, I. Danaee and M. G. Mahjani, *Electrochim Acta*, 52 (2007) 5437.
3. S. Shiomi, M. Miyake, T. Hirato and A. Sato, *Mater Trans*, 52 (2011) 1216.
4. S. Shiomi, M. Miyake and T. Hirato, *J Electrochem Soc*, 159 (2012) D225.
5. M. Miyake, H. Motonami, S. Shiomi and T. Hirato, *Surf Coat Tech*, 206 (2012) 4225.
6. M. Miyake, Y. Kubo and T. Hirato, *Journal of The Surface Finishing Society of Japan*, 64 (2013) 364.
7. M. Miyake, Y. Kubo and T. Hirato, *Electrochim Acta*, 120 (2014) 423.
8. M. Miyake, H. Fujii and T. Hirato, *Surf Coat Tech*, 277 (2015) 160.
9. Y. G. Zhao and T. J. VanderNoot, *Electrochim Acta*, 42 (1997) 3.
10. S. Z. El Abedin, E. M. Moustafa, R. Hempelmann, H. Natter and F. Endres, *Electrochem Commun*, 7 (2005) 1111.
11. J. K. Chang, S. Y. Chen, W. T. Tsai, M. J. Deng and I. W. Sun, *Electrochem Commun*, 9 (2007) 1602.
12. F. Endres, A. P. Abbott and D. R. MacFarlane, *Electrodeposition from ionic liquids*. 2008: Wiley-VCH.
13. L. Barchi, U. Bardi, S. Caporali, M. Fantini, A. Scrivani and A. Scrivani, *Prog Org Coat*, 67 (2010) 146.

14. A. Abbott, F. Qiu, H. Abood, M. Ali and K. Ryder, *Physical Chemistry Chemical Physics*, 12 (2010) 1862.
15. S. Takahashi, K. Akimoto and I. Saeki, *Journal of the Surface Finishing Society of Japan*, 40 (1989) 134.
16. A. P. Abbott, C. A. Eardley, N. R. S. Farley, G. A. Griffith and A. Pratt, *J Appl Electrochem*, 31 (2001) 1345.
17. Q. Liao, W. R. Pitner, G. Stewart, C. L. Hussey and G. R. Stafford, *J Electrochem Soc*, 144 (1997) 936.
18. F. H. Hurley and T. P. Wier, *J Electrochem Soc*, 98 (1951) 207.
19. F. C. Walsh and C. P. de Leon, *T I Met Finish*, 92 (2014) 83.
20. V. N. Tseluikin, *Protection of Metals and Physical Chemistry of Surfaces*, 52 (2016) 254.
21. W. Shao, D. Nabb, N. Renevier, I. Sherrington, Y. Fu and J. Luo, *J Electrochem Soc*, 159 (2012) D671.
22. B. M. Praveen and T. V. Venkatesha, *Appl Surf Sci*, 254 (2008) 2418.
23. P. Baghery, M. Farzam, A. B. Mousavi and M. Hosseini, *Surf Coat Tech*, 204 (2010) 3804.
24. G. Parida, D. Chaira, M. Chopkar and A. Basu, *Surf Coat Tech*, 205 (2011) 4871.
25. T. Deguchi, K. Imai, H. Matsui, M. Iwasaki, H. Tada and S. Ito, *Journal of Materials Science*, 36 (2001) 4723.
26. K. Murase, M. Ishida, I. Emori, E. Yamasue, T. Hirato and Y. Awakura, *Journal of The Surface Finishing Society of Japan*, 56 (2005) 692.
27. S. Spanou, A. I. Kontos, A. Siokou, A. G. Kontos, N. Vaenas, P. Falaras and E. A. Pavlatou, *Electrochim Acta*, 105 (2013) 324.
28. K. Ui, T. Fujita, N. Koura and F. Yamaguchi, *J Electrochem Soc*, 153 (2006) C449.
29. N. Fukumuro, Y. Usui, M. Komatsu, S. Yae and H. Matsuda, *Journal of The Surface Finishing Society of Japan*, 55 (2004) 355.
30. N. R. de Tacconi, C. A. Boyles and K. Rajeshwar, *Langmuir*, 16 (2000) 5665.
31. A. M. M. Jani, D. Losic and N. H. Voelcker, *Progress in Materials Science*, 58 (2013) 636.
32. W. Lee and S.-J. Park, *Chemical Reviews*, 114 (2014) 7487.
33. J. Fransaer, E. Leunis, T. Hirato and J. P. Celis, *J Appl Electrochem*, 32 (2002) 123.
34. T. Hirato, J. Fransaer and J. P. Celis, *J Electrochem Soc*, 148 (2001) C280.
35. J. A. Picas, A. Forn, E. Ruperez, M. T. Baile and E. Martin, *Plasma Processes and Polymers*, 4 (2007) S579.
36. J. Y. Hou and D. D. L. Chung, J*ournal of Materials Science*, 32 (1997) 3113.
37. S. C. Ferreira, A. Conde, M. A. Arenas, L. A. Rocha and A. Velhinho, *Materials*, 7 (2014) 8151.
38. M. Handel, D. Nickel, G. Alisch and T. Lampke, Materialwissenschaft Und Werkstofftechnik, 41 (2010) 737.
39. M. Shahid, *Journal of Materials Scienc*e, 32 (1997) 3775.
40. C. L. He, D. Y. Lou, J. M. Wang and Q. K. Cai, *Thin Solid Films*, 519 (2011) 4759.
41. S. Ono and N. Masuko, *Surf Coat Tec*h, 169 (2003) 139.
42. W. Lee and S. J. Park, *Chemical Reviews*, 114 (2014) 7487.
43. D. Crouse, Y. H. Lo, A. E. Miller and M. Crouse, *Appl Phys Lett*, 76 (2000) 49.
44. J. Tschirch, R. Dillert, D. Bahnemann, B. Proft, A. Biedermann and B. Goer, Research on *Chemical Intermediates*, 34 (2008) 381.